Chinese Chemical Letters 35 (2024) 109542

Contents lists available at ScienceDirect

Chinese Chemical Letters

journal homepage: www.elsevier.com/locate/cclet

Effect of coordination restriction on pressure-induced fluorescence evolution

Ziyou Zhang[a,b], Te Ji[c], Hongliang Dong[b], Zhiqiang Chen[b,*], Zhi Su[a,*]

[a] Jiangsu Collaborative Innovation Center of Biomedical Functional Materials, College of Chemistry and Materials Science, Nanjing Normal University, Nanjing 210046, China
[b] Center for High Pressure Science and Technology Advanced Research, Shanghai 201203, China
[c] Shanghai Synchrotron Radiation Facility, Shanghai Advanced Research Institute, Chinese Academy of Sciences, Shanghai 201204, China

ARTICLE INFO

Article history:
Received 22 December 2023
Revised 12 January 2024
Accepted 17 January 2024
Available online 24 January 2024

Keywords:
Coordination chemistry
High-pressure chemistry
FL-MOFs
High-pressure photoluminescent
Coordination restriction

ABSTRACT

The usage of flexible ligands in constructing MOF materials (FL-MOFs) has been widely studied due to its numerous advantages, including the structural diversity, polynuclear MOFs, transmitting magnetic exchanges, enantioselective separation, asymmetric catalysis, *etc*. However, the field still faces challenges in deeply understanding the effect of ligand configuration on the properties of these materials. Here, we employ a flexible aggregation-induced emission ligand (4,4′-((1*E*,1′*E*)-anthracene-9,10-diylbis(ethene-2,1-diyl))dibenzoic acid) with great mechanical stability to construct FL-MOFs to lock the ligand configuration to explore the pressure-induced evolution of the ligand with coordination restriction, involving changes in fluorescence and intermolecular interaction. *In-situ* high-pressure fluorescence, Raman, and FT-IR experiments have revealed that the intermolecular interaction of AIE-Mn-MOF with configuration restriction increased more rapidly than that of free AIE-L. This discovery offers valuable insights for synthesizing MOF materials with exceptional mechanical stability and significantly advances our understanding of the impact of coordination restriction in FL-MOFs on their response to external stimuli.

Metal-organic framework (MOF) materials are a new type of crystalline "soft" materials formed through the self-assembly of inorganic metal ions or metal clusters and organic ligands. The metal-ligand (M-L) coordinate bonds connecting metal and organic ligands grant MOF materials unique frame flexibility, resulting in high specific surface area, designable structure and function, and adjustable pore size, *etc*. [1–3], which present huge application prospects in the fields of gas adsorption and separation, catalysis, chemical sensing, proton conduction, and biomedicine [4–7]. The MOFs constructed based on flexible ligands (FL-MOFs) can accommodate the coordination preference of metal centers due to the ligands' flexibility, endowing FL-MOFs with dynamic properties in response to external stimuli [8–10]. However, the impact of the configuration of flexible ligands in FL-MOFs on the properties is not yet clear due to the configuration diversity of flexible ligands, which make it challenging to carry out a reasonable design.

9,10-Distyrylanthracene (DSA) and its derivatives are typical aggregation-induced emission (AIE) molecules with remarkable molecular flexibility, demonstrating advantages of high quantum efficiency of aggregated fluorescence, easily regulated molecular structure and excellent optical characteristics [11–14]. Furthermore, Tian and his collaborators systematically studied the luminescence characteristics of DSA derivatives under high-pressure through *in-situ* observation, revealed the mechanism of the evolution of aggregation structure and luminescence properties under pressure stimulation at the molecular level, which is the enhanced π-π interaction between adjacent anthracene rings leads to an increase in exciton coupling and orbital overlap between neighboring molecules, and also indicated that DSA derivatives exhibit outstanding stability under hydrostatic pressure [15–18]. These findings encourage the use of flexible DSA derivative molecules in constructing FL-MOFs to obtain MOF materials with superior mechanical stability and facilitate further studies on the effect of coordination restriction on ligand properties.

Here, we selected AIE material (4,4′-((1*E*,1′*E*)-anthracene-9,10-diylbis(ethene-2,1-diyl))dibenzoic acid) with significant framework flexibility under pressure as organic ligand to design and synthesize a new 2D AIE-Mn-MOF $[(Mn_3O_2)L_3(H_2O)_4(DMF)_2{\cdot}(Mn_3O_2)L_3(H_2O)_6]$. Under hydrostatic pressure generated by the diamond anvil cell (DAC), the fluorescence of AIE-Mn-MOF with coordination restriction effect showed red-shift and the weakened intensity. Meanwhile, AIE-Mn-MOF

* Corresponding authors.
E-mail addresses: chenzq@hpstar.ac.cn (Z. Chen), zhisu@njnu.edu.cn (Z. Su).

https://doi.org/10.1016/j.cclet.2024.109542
1001-8417/

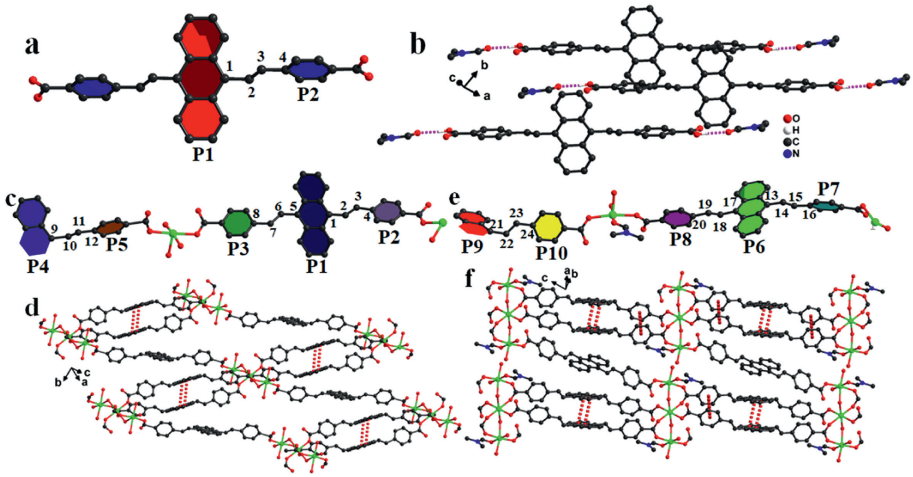

Fig. 1. (a) AIE ligand. (b) Crystal structure of AIE-L. (c, e) The asymmetric unit in AIE-Mn-MOF. (d, f) 2D layer based on $Mn_3O_2(H_2O)_6$ and $Mn_3O_2(DMF)_2(H_2O)_4$ cluster, respectively.

exhibited a blue-shift with almost constant intensity under shear force generated by grinding. For comparison, AIE ligand crystal represented red-shift under the action of two different forces. *In-situ* high-pressure fluorescence displayed that uncoordinated AIE ligand with higher flexibility possessed more mild response to pressure than AIE-Mn-MOF with coordination restriction effect. Furthermore, the fluorescence evolution mechanism was revealed by *in-situ* high-pressure Raman, FT-IR and PXRD experiments that pressure made the intermolecular π-π interaction of coordination locking increased rapidly. This work has not only clearly indicated the effect of coordination restriction on ligand properties, but also provided new insights for the synthesis of MOF materials with great mechanical stability.

AIE-L crystalized in the triclinic *P-1* space group, where the oxygen atom of the aldehyde group of the solvent molecule DMF formed a hydrogen bond with the hydroxyl part of the carboxyl group of ligand and existed in the structure (Figs. 1a and b). In the packing mode of the crystal, there was an absence π-π interaction between adjacent ligands, which effectively avoided non-radiative transitions. This is consistent with the strongest fluorescence of the AIE materials in the aggregate state.

The yellow crystal of AIE-Mn-MOF exhibited a typical 2D network consisting of two different 2D layers and crystallized in the triclinic *P-1* space group (Figs. 1c-f). In the 2D layer structure, the $(Mn_3O_2)(H_2O)_4(DMF)_2$ cluster was connected with two ligands, where the carboxyl group on one side of the ligand adopted the *syn-syn* coordination mode, while the other side was monodentate, forming a 1D chain. Compared to free AIE-L, the coordination locking led to a π-π weak interaction between the anthracene rings from adjacent ligands in the 1D chain, with a center distance of 3.685 Å. The 1D chain could further connect to the cluster to form a 2D layer through a ligand whose carboxyl groups at both ends were in a monodentate coordination mode. The other 2D layer was similar to the one above, except that the capping reagent DMF of the $(Mn_3O_2)(H_2O)_4(DMF)_2$ cluster was changed to H_2O, and there was no interaction between the two layers. Moreover, the remarkable differences in intramolecular conformations between free ligands and coordination-locked ligands were summarized in Table S3 (Supporting information), including the angle between the vinyl and anthracene ring, the angle between the vinyl and benzene ring, and the dihedral angle between the anthracene ring and benzene ring, which were compared in detail. It can be observed that the angle between vinyl and anthracene ring in AIE-Mn-MOF was greater than AIE-L, and the dihedral angle between the anthracene ring and benzene ring was smaller than AIE-L, indicating the coordination related distortion of the flexible ligand configuration. In addition, the twist degree of the ligand in the 2D layer where the capping reagent is water was greater than that of DMF.

AIE-L powder exhibited a strong absorption band at 300–500 nm and emitted intense yellow fluorescence at $\lambda_{max} = 575$ nm (Fig. S2 in Supporting information). In contrast, its solution in THF showed weak and wide orange-red emission at $\lambda_{max} = 622$ nm, which was due to conformational relaxation in the solution. Additionally, AIE-L aggregation in a THF/water (v/v = 1/9) solution exhibited aggregation-induced luminescence at $\lambda_{max} = 557$ nm with a blue shift and a 2.2-fold increase in intensity compared with the THF solution (Figs. S3 and S4 in Supporting information). Under grinding treatment, the AIE-L crystal exhibited a mechanical response where the fluorescence gradually red-shifted from 580 nm to 592 nm with a decrease in intensity (Fig. 2a). The PXRD of AIE-L after grinding was measured and compared with the initial PXRD to explain the mechanism of piezochromism, which revealed that the shear force made AIE-L crystal amorphous (Fig. S5a in Supporting information). Therefore, the reduced distance between molecules enhanced previously non-existent π-π interaction and non-radiative effects, causing the fluorescence to red-shift and the intensity to weaken [19,20].

Phase purity of AIE-Mn-MOF based on ligand with aggregation-induced emission was confirmed by PXRD, where the diffraction patterns of the synthesized complex were in agreement with the simulated counterparts (Fig. S5b in Supporting information). Even the diffraction pattern at 2θ of 6° comparing to the simulated one was missing, the high purity of AIE-Mn-MOF was no doubt, which may be resulted from the distinct test conditions and the sample preparation, such as the scanning speed, X-ray wavelength, and sample packing. Under visible light excitation at 480 nm, AIE-Mn-MOF emitted a strong yellow fluorescence similar to the AIE-L fluorescence pattern, indicated that the fluorescence mainly came from the ligand-to-ligand charge transfer (LLCT), and the weak blue shift might be attributed to the influence of the metal center (Fig. S6 in Supporting information) [21–23]. However, the fluorescence intensity of AIE-Mn-MOF was significantly lower than that of AIE-L, which is contrary to previous reports that the structure of the AIE fluorescent linkers are constrained in MOFs to effectively control their conformation, resulting in the adjust of the fluorescence energy and the improvement of the quantum yield [24–28]. For example, the PL quantum yield of PCN-94 (76.2%, air, r.t.) was far greater than its AIE ligand H_4ETTC (30.0%, air, r.t.) [24]. The flu-

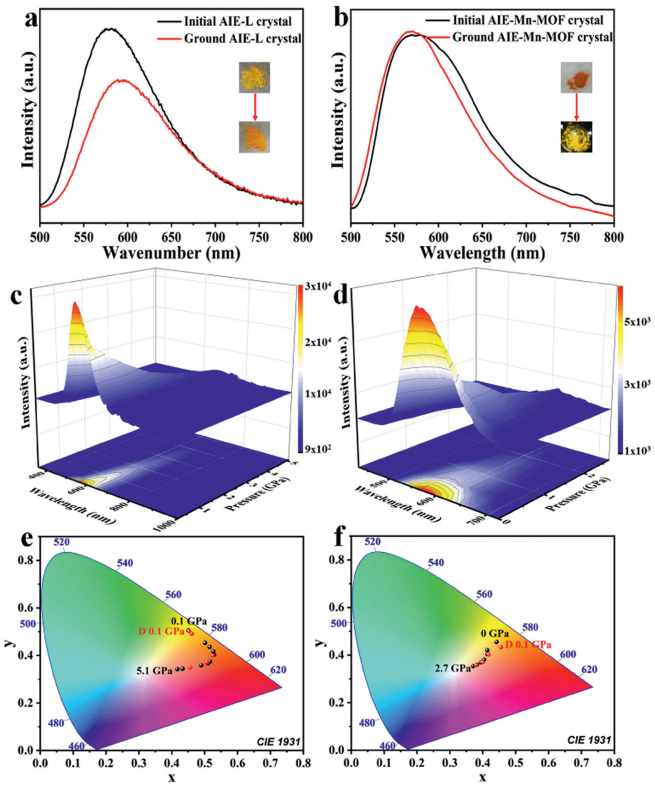

Fig. 2. (a, b) PL spectra of the initial, ground for AIE-L and AIE-Mn-MOF. (c, d) *In-situ* PL spectra upon the compression for AIE-L and AIE-Mn-MOF. (e, f) CIE coordinates upon the compression for AIE-L and AIE-Mn-MOF.

orescence intensity of AIE-Mn-MOF was lower than that of AIE-L, which was not only attributed to the non-radiative transition of the π-π interaction between flexible ligand and neighboring molecules in the AIE-Mn-MOF, but also due to the influence from Mn(II) ion centers [29–31]. Comparing with the ligand AIE-L, AIE-Mn-MOF had a blue shift after grinding, and maintained intensity (Fig. 2b). Moreover, PXRD of the grinded AIE-Mn-MOF was close to that of the as-prepared MOF, suggesting that the layered structures were perfectly preserved (Fig. S5b). Therefore, grinding triggered the local dynamics of the AIEgen rotors (local order disturbed) with slight rigidity after coordination to realize nondestructive mechanical stimulation response [32].

To further understand the piezochromic effect and the structure-property relationship, we investigated the pressure effects by diamond anvil cell (DAC), the DAC can provide a quantifiable hydrostatic pressure that has the distinct nature to the uncontrollable shear force generated by grinding, on the luminescence of AIE-L and AIE-Mn-MOF [33,34]. As the hydrostatic pressure increased from 1 atm to 5.1 GPa, the fluorescence emission of the AIE-L crystal gradually red shifted from 564 nm (yellow) to 668 nm (red) and the intensity dramatically decreased, showing a more pronounced effect than grinding (Figs. 2c and e). Meanwhile, the crystal emission color under 360 nm light varied from yellow to red with slightly faded in brightness, when above 5.1 GPa the emission signal was almost quenched (Fig. S7 in Supporting information). Correspondingly, the fluorescent spectra of AIE-L during decompression were recorded that the fluorescence of AIE-L almost returned to the initial state, and CIE coordinates, adsorption spectrum and crystal color also proceeded back to the initial state which signified that AIE-L had a reversible fluorescence response to pressure within 5.1 GPa (Fig. 2e, Figs. S7a and S11a in Supporting information). Additionally, to further verify its reversibility, we investigated the fluorescence spectra of three cycles of compression and decompression which illustrated that the fluorescence of AIE-L could be consistent with the initial state after each cycle (Fig. S8 in Supporting information). All the above results indicated that AIE-L crystal has great frame flexibility and can undergo reversible structural evolutions under pressure. However, under hydrostatic pressure the phenomenon of AIE-Mn-MOF was completely opposite to the shear force, that is, the fluorescence peak gradually red shifted from 590 nm to 618 nm as the hydrostatic pressure increased, and accompanied the intensity decreases (Figs. 2d and f). Comparing with free AIE-L, AIE-Mn-MOF with configuration locking exhibited the similar frame flexibility and the reversible fluorescence response to pressure (Figs. S9 and S10 in Supporting information), however, fluorescence intensity decreased faster and the redshift was less. The changes of fluorescence intensity and wavelength under compression, would be not only attributed to the strengthening of intermolecular interaction with coordination restriction, but also resulted from the decreased the distance between molecules and the enhanced non-existent π-π interaction and non-radiative effects [35–38].

To further explore the mechanism of pressure-induced electronic structural change and the effect of coordination on piezofluorochromism, the *in-situ* high-pressure FT-IR, Raman and UV–vis absorption spectra of AIE-L and AIE-Mn-MOF single crystal were investigated in DAC. Figs. 4a and b show the IR spectra of the AIE-L and AIE-Mn-MOF single crystal in the 650–1800 cm^{-1} range under different pressure, which mainly used to demonstrate molecular rotation [39,40]. By elevating the pressure, most of the IR peaks were blue-shifted indicating that the interatomic distances were decreased. However, the IR peak shape of AIE-Mn-MOF changed observably, suggesting that the strength of AIE-Mn-MOF intermolecular interaction with increased pressure was greater than that with AIE-L [40]. After the release of pressure, the IR peaks of the sample were similar to those initial patterns, suggesting that the pressure-enhanced intermolecular interactions were reversible [40].

The Raman peak at around 900–1000 cm^{-1} and 1550–1650 cm^{-1} assigned to C–H rocking vibration out of plane and C=C stretching vibration of vinyl or benzene ring skeleton, respectively [41,42]. With the elevated pressure, all the Raman peaks exhibited obvious blue shifts and gradually weaken in peak intensity, which indicated that the intermolecular interaction reinforced (Figs. 4c and d) [43,44]. In the approximate pressure range, the blue shift of represents C=C stretching Raman peaks (including P1, P2 and P3) in AIE-Mn-MOF was greater than that in AIE-L (Fig. 4e), which indicated that the pressure caused the original π-π interaction in AIE-Mn-MOF to enhance rapidly [45–47]. Meantime, no new peaks appeared during the entire compression process, revealing that no phase transition occurred [43]. When the pressure returned to atmospheric condition, all Raman peaks were restored to the initial state, demonstrating that the structural compression under pressure are completely reversible (Figs. S13 and S14 in Supporting information).

Additionally, the high-pressure absorption spectra of the AIE-L and AIE-Mn-MOF inside DAC were also measured. As shown in Fig. 3, the absorption spectra of both AIE-L and AIE-Mn-MOF smoothly broadened towards the redshift direction while the pressure increased, and the crystal also obviously changed from yellow to dark-red color under daylight. The calculated band gap for AIE-L and AIE-Mn-MOF indicated that AIE-Mn-MOF with coordination configuration locking was more sensitive to pressure than free AIE-L, where the band gap decreased from the initial 2.26 eV (0.1 GPa) to 1.71 eV (5.2 GPa) for AIE-Mn-MOF, in comparison to 2.42 eV (0 GPa) to 1.95 eV (6.2 GPa) for free AIE-L (Fig. 3). This tendency might be due to the rapid enhancement of intrinsic intermolecular interactions in the AIE-Mn-MOF structure under external pressure.

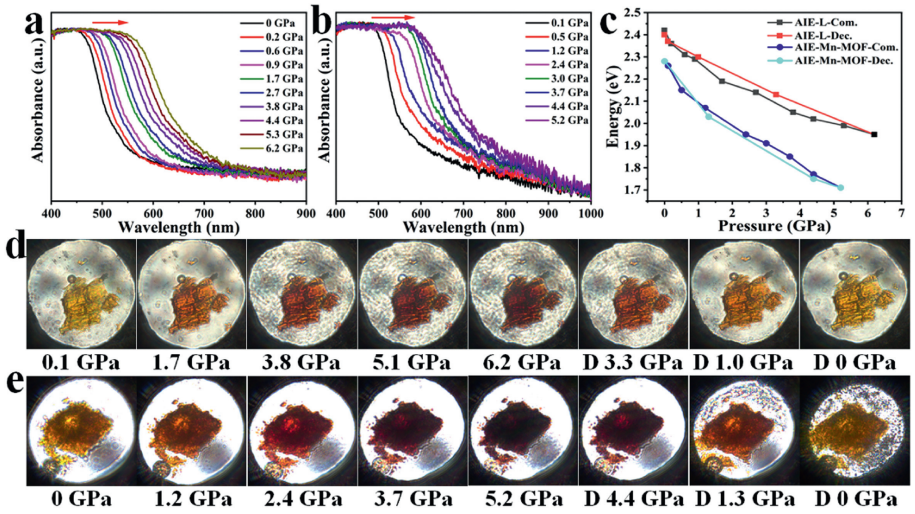

Fig. 3. (a, b) *In-situ* absorption spectra upon the compression for AIE-L and AIE-Mn-MOF. (c) Band gaps of AIE-L and AIE-Mn-MOF at different pressures. (d, e) Photographs under daylight at different pressures for AIE-L and AIE-Mn-MOF.

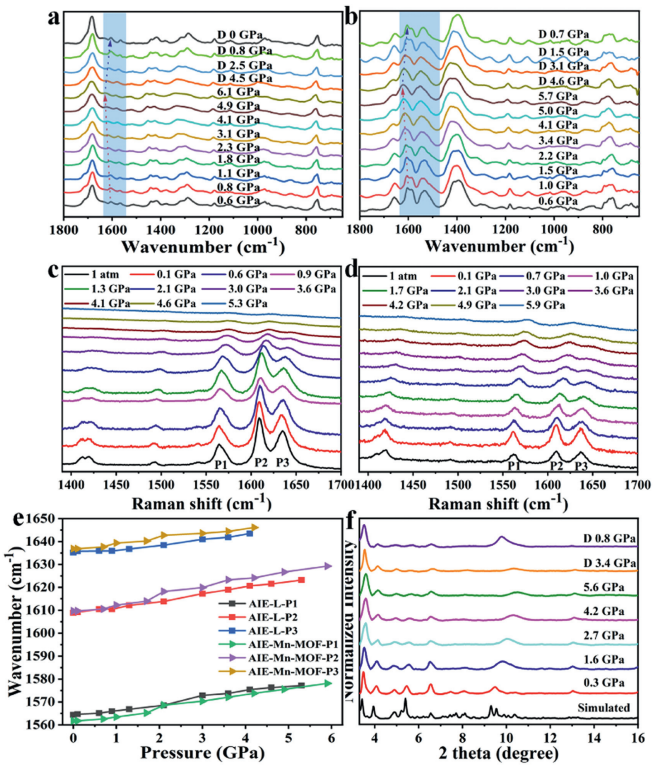

Fig. 4. *In-situ* FT-IR spectra upon the hydrostatic compression in DAC for (a) AIE-L and (b) AIE-Mn-MOF. *In-situ* high-pressure Raman spectra for (c) AIE-L and (d) AIE-Mn-MOF. (e) Pressure dependence of the Raman peak position for the sample. (f) High-pressure XRD patterns of AIE-Mn-MOF.

In order to further verify the structure-property relationship of AIE-Mn-MOF, we examined *in-situ* high-pressure XRD experiments in DAC from 1 atm to 5.6 GPa (Fig. 4f). With an increment in pressure, the mainly diffraction peaks were moved gradually to higher angles, indicating that AIE-Mn-MOF underwent a smooth compression, which was consistent with *in-situ* the spectral experimental data. The visible change in the peak width and peak shape was due to the reduction of the crystal grain size after the decompression [48]. Combined with the *in-situ* high-pressure FT-IR, Raman, absorption spectrum, and PXRD experiments, the results provided evidence that the different behavior of AIE-L and AIE-Mn-MOF under pressure could be attributed to the coordination-induced configuration locking of flexible ligands, which results in the distortion of the molecular configuration and the widespread intermolecular interactions within the structure.

In summary, we successfully designed and synthesized a new FL-MOF (AIE-Mn-MOF) based on flexible AIE ligand to explore the effect of coordination restriction on performance. In AIE-Mn-MOF, the ligand had a broad range of π-π interactions in the structure to satisfy the coordination requirements of the central metal, resulting in different properties compared to AIE ligands. Under hydrostatic pressure, free AIE-L demonstrated a greater red-shift (104 nm *vs.* 28 nm) and higher pressure responsive behavior (5.1 GPa *vs.* 2.7 GPa) comparing to the coordination restriction AIE-Mn-MOF. The mechanism underlying the difference in response to pressure was revealed by *in-situ* high-pressure Raman, UV–vis absorption, FT-IR and X-ray diffraction experiments that pressure made the intermolecular π-π interaction of coordination locking increased speedily. This work clearly demonstrated the impact of locking the flexible linker on luminescence performance through a series of *in-situ* experiments and combining the single crystal structure. Concurrently, these results confirmed that the transfer of mechanical property to MOF materials could be accomplished by the utilization of the mechanical stable linker.

Declaration of competing interest

The authors declare that they have no known competing financial interests or personal relationships that could have appeared to influence the work reported in this paper.

Acknowledgments

We thank the staffs of BL06B, BL15U1 beamlines at Shanghai Synchrotron Radiation Facility, Shanghai, People's Republic of China, for assistance during data collection. This work was supported by NSAF (No. U1530402) and Postgraduate Research & Practice Innovation of Jiangsu Province (No. KYCX22_1548). This work was also financially supported by the National Natural Science Foundation of China (Nos. 22277056, 21977052), the Distinguished Young Scholars of Jiangsu Province (No. BK20230006).

Supplementary materials

Supplementary material associated with this article can be found, in the online version, at doi:10.1016/j.cclet.2024.109542.

References

[1] Z. Jiang, X.H. Xu, Y.H. Ma, et al., Nature 586 (2020) 549–554.
[2] Z.J. Chen, P.H. Li, R. Anderson, et al., Science 368 (2020) 297–303.
[3] R.H. Dong, X.L. Feng, Nat. Mater. 20 (2021) 122–131.
[4] Z. Niu, X.L. Cui, T. Pham, et al., Angew. Chem. Int. Ed. 60 (2021) 5283–5288.
[5] L.J. Small, S.E. Henkelis, D.X. Rademacher, et al., Adv. Funct. Mater. 30 (2020) 2006598.
[6] H.H. Hu, Z.Y. Wang, L.Y. Cao, et al., Nat. Chem. 13 (2021) 358–366.
[7] A. Chandresh, X.J. Liu, C. Wöll, et al., Adv. Sci. 8 (2021) 2001884.
[8] Z.J. Lin, J. Lv, M.C. Hong, et al., Chem. Soc. Rev. 43 (2014) 5867–5895.
[9] J.P. Zhang, P.Q. Liao, H.L. Zhou, et al., Chem. Soc. Rev. 43 (2014) 5789–5814.
[10] Z. Chang, D.H. Yang, J. Xu, et al., Adv. Mater. 27 (2015) 5432–5544.
[11] J.T. He, B. Xu, F.P. Chen, et al., J. Phys. Chem. C 113 (2009) 9892–9899.
[12] J.B. Zhang, B. Xu, J.L. Chen, et al., J. Phys. Chem. C 117 (2013) 23117–23125.
[13] J.B. Zhang, S.Q. Ma, H.H. Fang, et al., Mater. Chem. Front. 1 (2017) 1422–1429.
[14] Q. Feng, N. Li, Z.Y. Zhang, et al., Chin. Chem. Lett. 34 (2023) 108439.
[15] B. Shao, R.H. Jin, A.S. Li, et al., J. Mater. Chem. C 7 (2019) 3263–3268.
[16] A.S. Li, Y.J. Liu, L. Han, et al., Dyes Pigments 161 (2019) 182–187.
[17] Y.J. Dong, B. Xu, J.B. Zhang, et al., Angew. Chem. 124 (2012) 10940–10943.
[18] Y.J. Liu, A.S. Li, S.P. Xu, et al., Angew. Chem. Int. Ed. 59 (2020) 15098–15103.
[19] Y.J. Liu, Q.X. Zeng, B. Zou, et al., Angew. Chem. Int. Ed. 57 (2018) 15670–15674.
[20] Q. Luo, L. Li, H.L. Ma, et al., Chem. Sci. 11 (2020) 6020–6025.
[21] C.M. Che, C.W. Wan, K.Y. Ho, et al., New J. Chem. 25 (2021) 63–65.
[22] C.M. Che, C.W. Wan, W.Z. Lin, et al., Chem. Commun. (2001) 721–722.
[23] F. Neve, A. Crispini, C.D. Pietro, et al., Organometallics 21 (2002) 3511–3518.
[24] Z.W. Wei, Z.Y. Gu, R.K. Arvapally, et al., J. Am. Chem. Soc. 136 (2014) 8269–8276.
[25] N.B. Shustova, B.D. McCarthy, M. Dincă, J. Am. Chem. Soc. 133 (2011) 20126–20129.
[26] N.B. Shustova, A.F. Cozzolino, S. Reineke, et al., J. Am. Chem. Soc. 135 (2013) 13326–13329.
[27] N.B. Shustova, T.C. Ong, A.F. Cozzolino, et al., J. Am. Chem. Soc. 134 (2012) 15061–15070.
[28] N.B. Shustova, A.F. Cozzolino, M. Dincă, J. Am. Chem. Soc. 134 (2012) 19596–19599.
[29] M.D. Allendorf, C.A. Bauer, R.K. Bhakta, R.J.T. Houk, Chem. Soc. Rev. 38 (2009) 1330–1352.
[30] Z.D. Lu, L.L. Wen, Z.P. Ni, et al., Cryst. Growth Des. 7 (2007) 268–274.
[31] H.F. Zhu, W. Zhao, T. Okamura, et al., New J. Chem. 28 (2004) 1010–1018.
[32] W.L. Shang, X.F. Zhu, T.L. Liang, et al., Angew. Chem. Int. Ed. 59 (2020) 12811–12816.
[33] Z.Y. Fu, K. Wang, B. Zou, Chin. Chem. Lett. 30 (2019) 1883–1894.
[34] Z.H. Wei, K. Zhang, C.K. Kim, et al., Chin. Chem. Lett. 32 (2021) 493–496.
[35] Y. Mu, F.Y. Cao, X.Y. Fang, et al., Adv. Optical Mater. 11 (2022) 2202402.
[36] X.J. Wang, T.H. Huang, L.H. Tang, et al., CrystEngComm 12 (2010) 4356–4364.
[37] Y. Mikata, Dalton Trans. 49 (2020) 17494–17504.
[38] X.T. Cai, Z.P. Xiong, J.L. Zhan, et al., Chem. Commun. 58 (2022) 10837–10840.
[39] S.Y. Li, Q. Wang, Y. Qian, et al., J. Phys. Chem. A 111 (2007) 11793–11800.
[40] S. Tong, J.H. Dai, J.M. Sun, et al., Nat. Commun. 13 (2022) 5234.
[41] Z. Gao, K. Wang, F.M. Liu, et al., Chem. Eur. J. 23 (2017) 773–777.
[42] X.D. Liu, A.S. Li, W.Q. Xu, et al., Phys. Chem. Chem. Phys. 20 (2018) 13249–13254.
[43] X.L. Guo, N.S. Zhu, S.P. Wang, et al., Angew. Chem. Int. Ed. 59 (2020) 19716–19721.
[44] Y.X. Dai, S.T. Zhang, H.C. Liu, et al., J. Phys. Chem. C 121 (2017) 4909–4916.
[45] J.A. Ciezak, T.A. Jenkins, Z.X. Liu, et al., J. Phys. Chem. A 111 (2007) 59–63.
[46] T.R. Park, Z.A. Dreger, Y.M. Gupta, J. Phys. Chem. B 108 (2004) 3174–3184.
[47] M. Dimitrievska, F. Oliva, M. Guc, et al., J. Mater. Chem. A 7 (2019) 13293–13304.
[48] W.W. Li, J.J. Feng, X.L. Zhang, et al., J. Am. Chem. Soc. 143 (2021) 20343–20355.